

# Mechanochemical Formation, Solution Rearrangements, and Catalytic Behavior of a Polymorphic Ca/K Allyl Complex

Ross F. Koby,<sup>[a]</sup> Alicia M. Doerr,<sup>[b]</sup> Nicholas R. Rightmire,<sup>[a]</sup> Nathan D. Schley,<sup>[a]</sup>  
William W. Brennessel,<sup>[c]</sup> Brian K. Long,<sup>[b]</sup> and Timothy P. Hanusa<sup>\*[a]</sup>

**Abstract:** Without solvents present, the often far-from-equilibrium environment in a mechanochemically driven synthesis can generate high-energy, non-stoichiometric products not observed from the same ratio of reagents used in solution. Ball milling 2 equiv.  $K[A']$  ( $A' = [1,3-(SiMe_3)_2C_3H_3]^-$ ) with  $Ca_2$  yields a non-stoichiometric calciate,  $K[CaA'_3]$ , which initially forms a structure (1) likely containing a mixture of pi- and sigma-bound allyl ligands. Dissolved in arenes, the compound rearranges over the course of several days to a

structure (2) with only  $\eta^3$ -bound allyl ligands, and that can be crystallized as a coordination polymer. If dissolved in alkanes, however, the rearrangement of 1 to 2 occurs within minutes. The structures of 1 and 2 have been modeled with DFT calculations, and 2 initiates the anionic polymerization of methyl methacrylate and isoprene; for the latter, under the mildest conditions yet reported for a heavy Group 2 species (one-atm pressure and room temperature).

## 1. Introduction

The fundamental organizing principles of the periodic table suggest that compounds containing metals of the same group and with similar ligands should display related properties. Hence Grignard-like reactivity was anticipated from organocalcium compounds when research on the latter started over a century ago.<sup>[1,2]</sup> Until the importance of metal coordination sphere saturation and kinetic stabilization were recognized, however, the multi-decadal efforts to extrapolate the chemistry of magnesium to its heavier congeners were largely unproductive.<sup>[3]</sup> It is now well documented that the coordination and organometallic chemistry of calcium, strontium, and barium differs significantly from that of magnesium analogues.<sup>[4]</sup> Calcium compounds in particular have been the subject of intense interest as initiators of polymerization,<sup>[5]</sup> hydrogenation,<sup>[6]</sup> and hydroelementation reactions,<sup>[7]</sup> and as promoters of nucleophilic alkylation.<sup>[8]</sup>

Central to the modern development of organo-Ca, -Sr, and -Ba chemistry has been the increasingly sophisticated use of large, sterically bulky ligands that provide hydrocarbon solubility and suppress undesirable behavior, such as ether cleavage or Schlenk-type ligand redistribution. Whole classes of organo-

alkaline-earth species, such as those possessing  $\pi$ -delocalized anions as ligands (e.g., cyclopentadienyl and allyl groups)<sup>[9]</sup> are now known that are relatively resistant to solvent attack, and are in fact frequently isolated as solvates. Such coordinated solvents can still affect subsequent reactivity, however. We have recently shown, for example, that the unsolvated  $\{[MgA'_2]_2\}$  ( $A' = 1,3-(SiMe_3)_2C_3H_3$ ) allyl complex is a modestly active initiator of methyl methacrylate polymerization, yielding isotactically enriched poly(methyl methacrylate) (PMMA).<sup>[10]</sup> The solvated  $[MgA'_2(thf)_2]$  complex, in contrast, is completely inactive for this purpose,<sup>[11]</sup> a likely consequence of the congestion of the coordination sphere by the bound thf ligands. Other examples of solvent-suppressed reactivity in Group 2 complexes are known.<sup>[8,12]</sup>

The potential inhibitory effect of coordinated solvents raises the countervailing possibility that complexes known to be active reagents or catalytic initiators *despite* the presence of coordinated solvents (e.g.,  $[CaA'_2(thf)_2]$  or  $[SrA'_2(thf)_2]$  for MMA polymerization)<sup>[11]</sup> might be more reactive in an unsolvated form. Of course, an unsolvated (and potentially coordinatively undersaturated) complex may dimerize or oligomerize, altering its reactivity, but in solution an active monomeric form could exist in equilibrium with a more highly coordinated and sterically crowded arrangement. This happens in the case of  $\{[MgA'_2]_2\} \rightleftharpoons 2 [MgA'_2]$ ,<sup>[13]</sup> and even with caveats about extrapolating from the behavior of magnesium to the heavier alkaline-earths, could occur in calcium or strontium systems as well (Figure 1).<sup>[10]</sup>

Ethers are widely used in the synthesis of organoalkaline-earth compounds, and form the most common solvates. Their removal from oxophilic metal centers can be challenging if not impossible, and the preparation of unsolvated species may require alternate synthetic procedures. Attempts to remove diethyl ether from the solvated  $[BeA'_2(Et_2O)]$  resulted in the compound's decomposition,<sup>[14]</sup> and unlike  $[MgA'_2(Et_2O)_2]$ , the

[a] R. F. Koby, N. R. Rightmire, N. D. Schley, Prof. T. P. Hanusa  
Department of Chemistry, Vanderbilt University  
Nashville, TN 37235 (USA)  
E-mail: t.hanusa@vanderbilt.edu

[b] A. M. Doerr, Prof. B. K. Long  
Department of Chemistry, University of Tennessee  
Knoxville, TN 37996–1600 (USA)

[c] Dr. W. W. Brennessel  
X-ray Crystallographic Facility, Department of Chemistry  
University of Rochester, Rochester, NY 14627 (USA)

Supporting information for this article is available on the WWW under <https://doi.org/10.1002/chem.202100589>

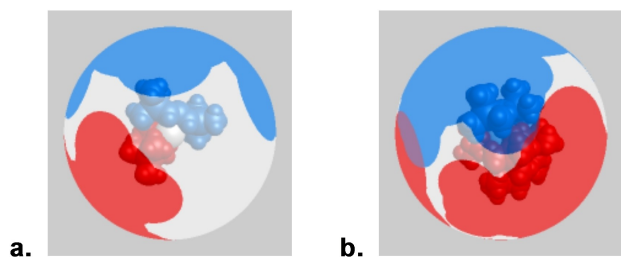


**Figure 1.** Visualization of the extent of coordination sphere coverage ( $G_{\text{complex}}$ ) calculated for: (a)  $[\text{CaA}'_2]$ , 71.2%; (b)  $\{[\text{CaA}'_2]\}_2$ , 90.4%. Optimized coordinates (B3PW91-D3BJ/def2TZVP) and the program Solid-G were used to predict the  $G_{\text{complex}}$  value; the latter represents the net coverage, so that regions of the coordination sphere where the projections of the ligands overlap are counted only once. For comparison, the values for  $[\text{MgA}'_2]$  and  $\{[\text{MgA}'_2]\}_2$  are 79.0% and 93.0%, respectively. The high  $G_{\text{complex}}$  values of the Ca and Mg dimers are suggestive of enough steric crowding to make partial dissociation in solution likely; this is known to occur for the Mg system.

$[\text{MgA}'_2(\text{thf})_2]$  analog could not be desolvated under prolonged vacuum.<sup>[13]</sup>

A direct way to circumvent strongly coordinating solvents is simply to avoid their use during synthesis. This can be done through solvent-free mechanochemical methods. Although long known, mechanochemistry in the form of grinding and ball milling has emerged in the past decade as a powerful synthetic tool, with solvent use minimized during synthesis.<sup>[15]</sup> Through these means, mechanochemistry has provided access to a range of compounds that could not be isolated because they are attacked by, or are unstable in, conventional reaction solvents.<sup>[16]</sup>

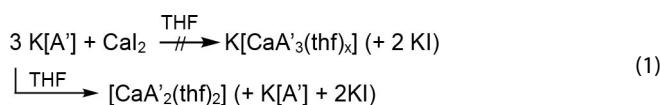
The synthesis of group 2 compounds frequently employs halide metathesis as a synthetic method, and under mechanochemical conditions reagent stoichiometry is not a reliable guide to the composition of products. During grinding, reagents are placed in conditions far from equilibrium, and the reaction speed may not allow for equilibration or redistribution to occur. In addition, the high reagent concentration and the potential coordinative undersaturation of the expected products can lead to the isolation of unanticipated products. For instance, '-ate'-type species can form instead of the intended neutral complexes, as when milling two equivalents of  $\text{K}[\text{A}']$  with  $\text{MgCl}_2$  produces  $\text{K}_2[\text{MgA}'_4]$  rather than the expected  $[\text{MgA}'_2]$ .<sup>[10]</sup>

It should be noted that the mechanochemical generation of -ate species, should it occur, may be an advantage for the production of catalytically useful compounds, as initiator activity in anionic polymerizations has been correlated with net negative charges on the complex.<sup>[17]</sup> Neither the neutral  $[\text{Mg}(\text{C}_3\text{H}_5)_2]$  complex nor the cationic species  $[\text{Mg}(\text{C}_3\text{H}_5)_2(\text{thf})_2]^+$  will initiate butadiene polymerization, for example.<sup>[17]</sup> The heavier species  $[\text{Ca}(\text{C}_3\text{H}_5)_2]$  will, however, and the heterometallic complex  $\text{Ca}[\text{Mg}(\text{C}_3\text{H}_5)_4]$  species is even more active, a difference associated with the dianionic charge on the magnesiate. If this is the case, calciate- or strontiate-based initiators ( $[\text{Ca}(\text{allyl})_3]^-$ ,  $[\text{Sr}(\text{allyl})_3]^-$ ) may possess higher levels of activity than their neutral counterparts. Described here are the results of the

search for an unsolvated calcium allyl, the solvent-free mechanochemical synthesis of a bulky allyl calciate that in its initially isolated form requires arene solvation for stability, and that in its more thermodynamically stable form displays reactivity as a polymerization initiator under mild conditions.

## 2. Results and Discussion

The known neutral complex  $[\text{CaA}'_2(\text{thf})_2]$  is a product of solution-based chemistry,<sup>[18]</sup> and attempting to avoid the use of ethers to generate an unsolvated  $[\text{CaA}'_2]$  complex by using toluene as a solvent is unsuccessful.<sup>[19]</sup> Furthermore, an effort to prepare a bulky allyl calciate in THF solution with the use of a 3:1 ratio of the potassium allyl to calcium iodide (equation 1) yielded only the neutral complex.<sup>[11]</sup>



Allyl substitution on the calcium center may stop at the bis (allyl) stage as a consequence of a third allyl's inability to dislodge the strongly coordinating THF.

A mechanochemical approach to generating the neutral allyl complex was then attempted. Grinding a mixture of  $\text{K}[\text{A}']$  and  $\text{CaI}_2$  (2:1 equivalents) for 15 minutes at 600 RPM in a planetary ball mill leaves a highly air-sensitive pale-yellow powder that is somewhat soluble in toluene. Filtering a toluene extract through a fine porosity glass frit yields a transparent yellowish-orange solution. Drying under vacuum leaves an orange oil that eventually solidifies. An  $^1\text{H}$  NMR study of the oil indicated the presence of apparently  $\pi$ -bound  $\text{A}'$  ligands, and the pattern of 2 singlets (from TMS), 1 doublet (from H1 and H3), and 2 triplets (from H2) was originally attributed to an allyl calcium species with multiple allyl environments but accidentally overlapping doublets.

Systematic variation of reaction conditions revealed that there were two products generated whose formation could be changed by varying the grinding time. One of the products (1) is preferentially formed at short milling times (5–10 min) and the other (2) is produced after extended milling (15–20 min). Outside the mill, 1 spontaneously transforms into 2 either in the solid state (over 3 days) or in hydrocarbon solution (from minutes to days). The transformation is accompanied by a shift and intensification of color from yellow to red-orange, but with no other obvious signs of decomposition (e.g., formation of a precipitate, change in solubility), and it seems that 1 is a metastable form of 2 (Figure 2). Elemental analysis of 2 is consistent with the formula  $\text{K}[\text{CaA}'_3]$ , which is not the stoichiometrically expected product from the reaction. In an attempt to optimize its yield, a 3:1 combination of  $\text{K}[\text{A}']$  and  $\text{CaI}_2$  was ground together, but the additional  $\text{K}[\text{A}']$  did not appear to participate in the reaction, and could be identified with  $^1\text{H}$  NMR spectroscopy separately from  $\text{K}[\text{CaA}'_3]$ .  $\text{K}[\text{CaA}'_3]$  was also the only identifiable product ( $^1\text{H}$  NMR) from a 1:1 grind of  $\text{K}[\text{A}']$  and  $\text{CaI}_2$ . Clearly  $\text{K}[\text{CaA}'_3]$  is the preferred product from these

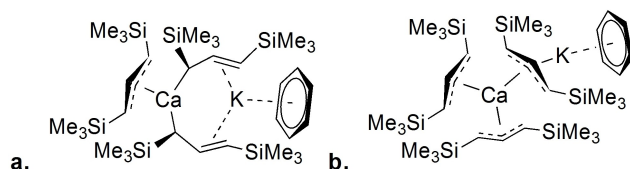


**Figure 2.** Proposed structures of arene-solvated versions of  $K[CaA'_3]$ : (a) **1** ( $[C_6H_6 \cdot K[Ca(\eta^3-A')(\eta^1-A')_2]]$ ), the initially isolated product; (b) **2** ( $[C_6H_6 \cdot K[Ca(\eta^3-A')_3]]$ ), the form obtained after rearrangement. See the computational results section for rationalizations of these structures.

reactions, much as  $K[BeA'_3]$  is found to be the only product regardless of whether 1:1, 2:1, or 3:1 ratios of  $K[A']$  and  $BeCl_2$  are ground.<sup>[20]</sup>

Compounds **1** and **2** have distinctive  $^1H$  NMR spectra (see Table 1), and although the ligands appear  $\eta^3$ -bound,  $A'$  anions on electropositive metals are known to be fluxional, and even those found to be  $\eta^1$ -bound in the solid state (e.g., on  $Be$ ,<sup>[20]</sup>  $Zn$ ,<sup>[21]</sup>  $Al$ ,<sup>[16a]</sup>  $Ga$ <sup>[22]</sup>) appear  $\pi$ -bound in solution. The most obvious difference between **1** and **2** is the chemical shift of the central hydrogen on the  $A'$  ligand, which appears as a triplet, owing to coupling with the two terminal hydrogens. The shift in **1** ( $\delta = 7.25$ ,  $^1J_{H-H} = 16$  Hz) moves upfield in **2** ( $\delta = 6.99$ ,  $^1J_{H-H} = 16$  Hz). In allyl complexes containing the  $A'$  ligand, a shift for the central hydrogen more downfield than  $\delta = 7.0$  is unusual; for example, it appears at  $\delta = 6.69$  for  $K[A']$  ( $\eta^3$ -bound) and at  $\delta = 6.83$  for  $[MgA'_2(thf)_2]$  ( $\eta^1$ -bound).<sup>[13]</sup> Although not completely diagnostic, shifts near or greater than  $\delta = 7.0$  have been observed before in  $A'$ -ate complexes that have  $\sigma$ -bound ligands in the solid state (Table 1). It is possible, in fact likely, that a complex featuring one or more  $\sigma$ -bonded ligands is present here, a point discussed in the computational section.

Compound **1** has a complex interaction with solvents. In anything other than neat arenes, the rate of conversion of **1** into **2** is rapid. Even in a 90:10 ( $C_6D_6$ ):(hexanes) mixture, conversion to **2** occurs quickly (<10 min). Not surprisingly, attempts to crystallize **1** by layering mixtures of hexane, toluene, and/or  $(SiMe_3)_2O$ , or by evaporation from hexanes or  $(SiMe_3)_2O$  inevitably yields crystals of **2**. Even from a neat arene solvent, crystallization that is slow enough to form well-defined crystals always produces only **2**.

An  $^1H$  NMR study was conducted over four days at 6-h intervals to study the rate of transformation as a function of time and solvent composition. The results in neat  $C_6D_6$  are detailed in the Supporting Information (Figure S13), but in

**Table 1.**  $^1H$  NMR shifts in  $C_6D_6$  for selected electropositive  $[A']$  complexes.

Complex	TMS (s)	$H_{1,3}$ ( $^1J_{H-H}$ , Hz)	$H_2$ ( $^1J_{H-H}$ , Hz)	Ref.
<b>1</b>	0.34	3.33 (16)	7.25 (16)	[a]
<b>2</b>	0.21	3.32 (16)	6.99 (16)	[a]
$K[BeA'_3][b]$	0.22	3.21 (br)	6.97 (16)	[20]
$Na[ZnA'_3][b]$	0.16	4.00 (br)	7.59 (16)	[21]
$K[ZnA'_3][b]$	0.23	3.42 (15)	7.05 (15)	[21]
$K[A'][c]$	0.23	2.78 (16)	6.69 (16)	[26]

[a] This work. [b]  $\eta^1$ -Bound in the solid state. [c]  $\eta^3$ -Bound in the solid state.

summary, there is a long induction period for the transformation of **1** to **2**, but once it begins, it is fairly rapid. Specifically, a sample of **1** appears unchanged for slightly less than two days (42 h), but by 48 h, the distinctive resonances of **2** are clearly evident (ca. 15% of the total). Over the next 30 h (a total of 78 h since the start), virtually complete conversion to **2** occurs. Such behavior has some of the hallmarks of an autocatalytic reaction,<sup>[23]</sup> but the difficulty in characterizing the form(s) of **1** in solution (see below) means that detailed analysis of this point would not be justified.<sup>[24]</sup>

In toluene, the UV-vis spectrum of **2** displays a broad absorbance at 316 nm, tailing into the visible region (see the Supporting Information). The absorbance is probably associated with transitions involving the allyl anion.<sup>[25]</sup>

## 2.1. Crystallographic results

Compound **2** crystallizes from hexanes within two days as pale yellow, nearly colorless blocks with the composition of  $\{K[CaA'_3]\}_n$  (Figure 3). The whole comprises a coordination polymer with the three  $A'$  ligands  $\eta^3$ -bound to calcium, one of which is terminal, and two in  $\mu_2$ - $\eta^3$ : $\eta^3$  modes. The  $K^+$  counterion interacts with two of the  $A'$  ligands, also in a  $\mu_2$ - $\eta^3$ : $\eta^3$  mode. Around the calcium, the allyl ligands are arranged in an irregular fashion, with Ca–C distances ranging from 2.573–2.752 Å, with an average of 2.67 Å. Despite the bond length variation, partially a result of the mix of terminal and bridging allyls, the average distance is similar to that found in  $[CaA'_2(thf)_2]$  (2.654(5) Å), which reflects the same formal coordination number of calcium (6). The K–C distances span a large range from 2.92–3.33 Å, averaging to 3.12 Å.

The coordination polymer chains persist in the solid state even with intercalated solvent molecules. A second crystal form of the calciate (**2b**) was obtained when a  $C_6D_6$  solvate crystallized slowly from a sample in an NMR tube. Its gross structure is

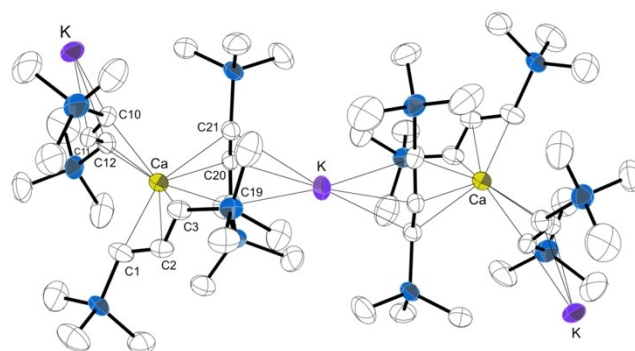


**Figure 3.** Thermal ellipsoid plot (50% level) of a portion of the coordination polymer of  $\{K[CaA'_3]\}_n$  (**2<sub>n</sub>**). Hydrogen atoms have been removed for clarity. Selected bond distances (Å) and angles ( $^\circ$ ): Ca–C1, 2.643(3); Ca–C2, 2.672(3); Ca–C3, 2.649(3); Ca–C10, 2.642(3); Ca–C11, 2.573(3); Ca–C12, 2.600(16); Ca–C19, 2.750(15); Ca–C20, 2.715(3); Ca–C21, 2.752(3); K–C19, 3.012(16); K–C20, 3.103(7); K–C21, 3.327(7); Ca...K, 5.055(8); C1–C2–C3, 128.1(5), C10–C11–C12, 128.8(5), C19–C20–C21, 130.6(5), Ca...K...Ca', 175.2, K...Ca...K', 122.3.

the same as **2**, comprising the coordination polymer with a terminal A' ligand on calcium, and the other two allyls bridging between calcium and potassium (Figure 4). In **2b**, the polymer chains have moved apart, generating cavities as large as 156 Å<sup>3</sup> that are filled with benzene. The closest C<sub>benzene</sub>...Me—Si contact is at 3.78 Å, roughly the sum of appropriate van der Waals radii (1.7 Å<sub>arene ring</sub> + 2.0 Å<sub>Me</sub>).<sup>[27]</sup>

A further example of the stability of the {K[CaA'<sub>3</sub>]<sub>n</sub>} chains was obtained when **2** was crystallized more slowly from commercial hexanes. The resulting iridescent rhombi (**2c**) were found to have grown in the polar space group P2<sub>1</sub>, different from that for **2** (P2<sub>1</sub>/m) or **2b** (P2<sub>1</sub>/n). The crystals of **2c** incorporate methylcyclopentane into the lattice as {K[CaA'<sub>3</sub>]·C<sub>5</sub>H<sub>9</sub>Me}<sub>n</sub>; the alicycle is a common component of hexanes.<sup>[28]</sup> The general connectivity is not in doubt, with the same {CaA'<sub>3</sub>-(μ-K)-CaA'<sub>3</sub>}<sub>n</sub> motif found in **2** and **2b**, but owing to several crystallographic issues, further discussion of **2c** is not warranted (see the Supporting Information for figures).

## 2.2. Computational results

The formation of **1** provides an unusual glimpse into a mechanochemically generated, relatively long-lived, but fundamentally transient complex.<sup>[29]</sup> Such species are becoming increasingly recognized features of mechanochemical synthesis, and their appearance and transformations have been followed in reactions that generate organic products,<sup>[30]</sup> MOFs,<sup>[31]</sup> and coordination polymers,<sup>[32]</sup> and studied with the use of synchrotron-based spectroscopy,<sup>[32,33]</sup> time-resolved *in situ* Raman spectra,<sup>[34]</sup> or combination techniques.<sup>[35]</sup> Although **1** and **2** can be distinguished with NMR spectra, and the **1**→**2** conversion can be suppressed for several days with appropriate solvent choice, we were interested in developing computational models for the two species that might help us understand their nature and conversions more fully.

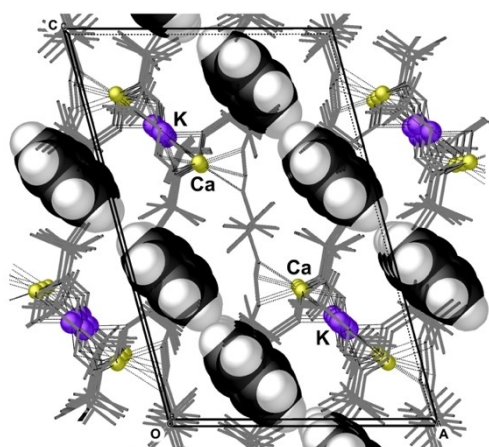


**Figure 4.** Portion of the coordination polymer of {K[CaA'<sub>3</sub>]·C<sub>6</sub>D<sub>6</sub>]<sub>n</sub>} (**2b**), projected down the crystallographic *b* axis. Carbon-carbon and carbon-silicon bonds are shown as sticks, and interstitial benzene molecules are displayed with space-filling parameters. A thermal ellipsoid plot of **2b** is available in the Supporting Information (Figure S4).

Several guiding principles were used during the construction of the models: 1) the base formulas of **1** and **2** are the same, i.e., K[CaA'<sub>3</sub>], and they are presumed to be monomeric in solution; 2) there is some sigma-bonding character to the allyls in **1**, even though fluxionality makes the allyls appear to be π-bound; 3) in solution, interaction with arenes slows, but does not ultimately prevent the conversion of **1** to **2**. This suggests the operation of a cation-π interaction of the arenes with one or both of the metals in both forms of the complex.<sup>[36]</sup> Hence a mechanism that involves the (temporary) displacement of arene(s) from **1**, thus allowing rearrangement to **2** to occur would seem to be likely. Certainly more than one solvent molecule surrounds **1** and **2** when they are in solution, and the application of a solvation model (e.g., PCM<sup>[37]</sup>) might be appropriate in this context, but preliminary calculations with this approach suggested that explicit modeling of the metal-arene interaction was critical, and we opted to use a discrete solvent approach.

A model for the solution structure of **2** was the most straightforward, as we assumed it could be represented as a fragment of the solid-state coordination polymer. A calcium center, three surrounding η<sup>3</sup>-A' ligands, and a K<sup>+</sup> ion on the opposite face of one of allyls served as the basis of the model. A single C<sub>6</sub>H<sub>6</sub> molecule was placed in a capping position over the potassium (2·C<sub>6</sub>H<sub>6</sub>; Figure 1b). A DFT calculation with the B3PW91-D3BJ/def2SVP combination (the level of calculation used for all molecules in this section) found the structure to be a minimum on the potential energy surface. Any comparisons with the crystal structure of **2** must be made with some caution, as there are two terminal A' ligands in this model for **2**, and only one that is bridging, the reverse of the case in the coordination environment around Ca<sup>2+</sup> in the solid-state structure. The K<sup>+</sup> ion is coordinated by only one anionic ligand in the model, as distinct from two in the crystal. Nevertheless, several parameters compare well between the model and the crystal structure. The Ca–C distances average to 2.63 Å, slightly shorter than in the solid state (2.67 Å). The K<sup>+</sup>–C(allyl) distance averages to 2.99 Å, notably shorter than in the crystal structure (3.15 Å), but a reasonable consequence of its being bound to only one anionic ligand, rather than two as in the polymer. In the model, there is auxiliary coordination to the K<sup>+</sup> by a neighboring CH<sub>3</sub> group (3.17 Å), and of course by the C<sub>6</sub>H<sub>6</sub> ring, with a K<sup>+</sup>...centroid distance of 3.22 Å. The latter is comparable to the 3.25 Å K<sup>+</sup>...ring centroid distance calculated for the monomeric [(C<sub>6</sub>H<sub>6</sub>)KA'] complex (see the Supporting Information, Figure S12).

A model for **1** was not as easily constructed as for **2**. To accommodate the presence of η<sup>1</sup>-allyls, an initial guess was a structure related to K[MA'<sub>3</sub>] (M = Be,<sup>[20]</sup> Zn,<sup>[21]</sup> Sn<sup>[16a]</sup>), in which the allyl ligands adopt a μ<sub>2</sub>-η<sup>1</sup>:η<sup>2</sup> bonding mode, being σ-bonded to the divalent metal and with cation-π interactions between the K<sup>+</sup> ion and the double bonds of the allyl ligands. An additional cation-π interaction would exist between K<sup>+</sup> and an arene ring capping one end (Figure 5a). A Ca<sup>2+</sup> center coordinated by all-η<sup>1</sup>-bonded allyls could explain the instability of **1** over time, a consequence of the strong preference for η<sup>3</sup>-over η<sup>1</sup>-bound allyl ligands on calcium.<sup>[38]</sup> A calculation for the

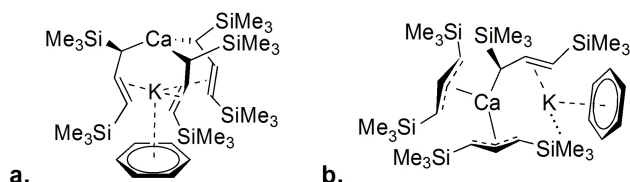


**Figure 5.** Structures of proposed but rejected models for **1**; (a) a  $C_3$ -symmetric version, in which the allyl ligands adopt a  $\mu_2\text{-}\eta^1\text{:}\eta^2$  arrangement; (b) a mixed hapticity version with two  $\eta^3$ - and one  $\eta^1$ -allyl on Ca. The preferred model for **1** is found in Figure 2a.

5a model of **1** found it to be a local minimum, and the average Ca–C bond length of 2.514 Å is similar to the crystallographically characterized calcite  $\text{K}[\text{Ca}\{\text{CH}(\text{SiMe}_3)_2\}_3]$  (2.50(1) Å).<sup>[39]</sup>

Though initially appealing, this structure was ultimately considered not the most likely model for  $1 \cdot \text{C}_6\text{H}_6$ . The  $C_3$ -symmetric  $\text{K}[\text{MA}'_3]$  framework has never been observed when M is a highly electropositive metal; even Mg ( $\chi = 1.31$ ) does not form such a complex.<sup>[10]</sup> In the present case, the incorporation of Ca ( $\chi = 1.00$ ) would appear to have even less chance of success. Furthermore, the 5a model offers no obvious mechanism for the experimentally observed arene stabilization. Reoptimization of the 5a structure without the benzene increases the separation between the  $\text{Ca}^{2+}$  and  $\text{K}^+$  by 0.47 Å, but the all  $\sigma$ -bonded framework is left otherwise intact (see the Supporting Information for details).

Of course, all the allyls in **1** need not be  $\sigma$ -bonded to  $\text{Ca}^{2+}$ , and it would be stabilizing if any of the ligands were  $\pi$ -bonded to  $\text{Ca}^{2+}$ . Two additional models for **1** with mixed hapticity allyl ligands were thus considered; one with two  $\eta^3\text{-A}'$  and one  $\eta^1\text{-A}'$  ligand (Figure 5b) and another with one  $\eta^3\text{-A}'$  and two  $\eta^1\text{-A}'$  ligands (Figure 2a). In both cases, the  $\text{K}^+$  is coordinated by the double bond(s) of the  $\eta^1$ -allyl(s) and an associated  $\text{C}_6\text{H}_6$ . Although the interaction of the  $\text{K}^+$  with the allyl ligands is not the same, the proposed 2a structure has similarities with the known mixed hapticity  $\text{K}_2[\text{Mg}(\eta^3\text{-A}')(\eta^1\text{-A}')_3]$  magnesiate.<sup>[10]</sup>

Both calcium structures are minima on their respective energy surfaces and are lower in energy than the all- $\sigma$  bound version (5a). The 5b version by itself, with its two  $\eta^3\text{-A}'$  ligands on  $\text{Ca}^{2+}$ , is lower in energy than the preferred Figure 2a alternative ( $\Delta G^\circ = -6.1 \text{ kcal mol}^{-1}$ ), but despite the coordination to the  $\text{K}^+$  by a neighboring  $\text{CH}_3$  group (3.07 Å) and  $\text{C}_6\text{H}_6$  ring, the potassium remains coordinatively undersaturated. Removal of the  $\text{C}_6\text{H}_6$  still leaves  $\text{Ca}^{2+}$  with  $(\eta^3)_2(\eta^1)$ -coordinated A' ligands, but the  $\text{K}^+$  now has a more complicated bridging interaction with the allyls, and is approached by two  $\text{CH}_3$  groups (both at 3.10 Å; the Supporting Information presents a figure of this configuration (S10)). The undersaturation at potassium is probably the reason that the loss of  $\text{C}_6\text{H}_6$  is endothermic by  $+11.8 \text{ kcal mol}^{-1}$  ( $\Delta H^\circ$ ), leading to a small but positive free energy change ( $\Delta G^\circ = +3.2 \text{ kcal mol}^{-1}$ ); the resistance to arene loss makes it an unlikely candidate for the structure of **1**.

In the optimized structure of  $1 \cdot \text{C}_6\text{H}_6$  with  $(\eta^3)(\eta^1)_2$ -coordinated allyls on Ca (Figure 2a), the average  $\text{K}^+ \dots \text{C}$  distance to the double-bonded carbons of the two  $\eta^1$ -bonded allyls is

3.00 Å, which is slightly shorter than the comparable distances in  $\text{K}[\text{ZnA}'_3]$  (3.08 Å) or  $\text{K}[\text{BeA}'_3]$  (3.05 Å), and consistent with the interaction's energetic importance.

When the  $\text{C}_6\text{H}_6$  is removed and the structure reoptimized, a process that involves only a small free energy change ( $\Delta G^\circ = -1.7 \text{ kcal mol}^{-1}$ ) (Figure S11), one of the  $\sigma$ -bonded allyls becomes  $\pi$ -bonded; the average Ca–C distances for the two  $\eta^3\text{-A}'$  ligands is 2.62 Å, almost identical to the distance in the calculation for the monomeric **2** (2.63 Å), and the  $\pi$ -electrons in both ligands are delocalized. There are limits to what can be expected from a gas-phase approximation, of course, and the third allyl is still  $\eta^1$ -bound to the Ca (2.60 Å), but the  $\text{K}^+$  is now  $\eta^3$ -bonded to the ligand, with an average K–C distance of 2.99 Å. Owing to the substantial rearrangement that occurs on removal of the  $\text{C}_6\text{H}_6$ , we favor this mixed hapticity species (Figure 2a) as the most likely model of those considered for  $1 \cdot \text{C}_6\text{H}_6$ . The conversion of the preferred solvated models ( $1 \cdot \text{C}_6\text{H}_6 \rightarrow 2 \cdot \text{C}_6\text{H}_6$ ) is spontaneous by  $7.7 \text{ kcal mol}^{-1}$  ( $\Delta G^\circ$ ).

### 2.3. Polymerization results

Group 1 and 2 metal (trimethylsilyl)allyl complexes are known to be initiators for the polymerization of methyl methacrylate (MMA),<sup>[11,26,40]</sup> and it was expected that **2** would likely follow suit. The MMA polymerization activity of **2** was evaluated in toluene (0.5 M) at several temperatures, as detailed in Table 2. In order to obtain tractable data, polymerizations were conducted at high monomer:initiator ratios (1000:1). Regardless of temperature, polymer yields were low to moderate (22–49%), displayed high dispersities ( $D = 8.2\text{--}10.4$ ), and were isotactically enriched (see the Supporting Information). It was noted that previous studies have shown that the related initiator  $\text{K}[\text{A}']$  produces only atactic PMMA (entry 5),<sup>[26,41]</sup> whereas  $[\text{CaA}'_2(\text{thf})_2]$  also generates isotactically enriched PMMA in toluene.<sup>[11]</sup> Although the temperature dependence of anionic polymerizations is known to be small relative to cationic systems,<sup>[42]</sup> an expected increase in turnover frequency (TOF) was observed for polymerizations conducted at  $0^\circ\text{C}$  (entries 1–2), which may be a result of the suppression of deleterious “backbiting” reactions and initiator degradation.<sup>[43]</sup> However, the TOF of polymerizations conducted at  $-78^\circ\text{C}$  are essentially the same as those at  $25^\circ\text{C}$ , as has been observed when other ion pairs are involved in propagation.<sup>[44]</sup>

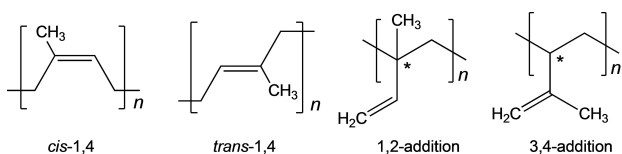
The broad PMMA dispersity observed when using initiator **2** is similar to those previously observed when using Grignard reagents as initiators in MMA polymerizations.<sup>[45]</sup> Such compounds are subject to Schlenk equilibria ( $2 \text{ RMgX} \rightleftharpoons \text{R}_2\text{Mg} + \text{MgX}_2$ ), which means there are multiple active sites and the likelihood of side reactions, both of which may complicate initiation and propagation during the polymerization. A directly analogous rearrangement (i.e.,  $\text{K}[\text{CaA}'_3] \rightleftharpoons \text{K}[\text{A}'] + [\text{CaA}'_2]$ ) is probably not relevant here, as the low solubility of  $\text{K}[\text{A}']$  would shift the equilibrium far to the right, removing  $\text{K}[\text{CaA}'_3]$  from solution. Instead, we hypothesize that varying amounts of aggregation may be occurring that could contribute to the broad dispersities observed.

**Table 2.** <sup>1</sup>H polymerization results with **2**.<sup>[a]</sup>

(A) Polymerization of MMA <sup>[a]</sup>										
Entry	Initiator	Mono/ cat	Temp (°C)	Time	Yield (%)	TOF (min <sup>-1</sup> )	M <sub>n</sub> (g/ mol)	Đ	Tacticity <sup>[c]</sup>	Ref.
1	K[CaA' <sub>3</sub> ] ( <b>2</b> )	1000	RT	8 min	22	27	63,600 <sup>[b]</sup>	8.44 <sup>[b]</sup>	69/22/9 (isotactic enriched)	this work
2	K[CaA' <sub>3</sub> ] ( <b>2</b> )	1000	0	8 min	49	61	75,700 <sup>[b]</sup>	8.25 <sup>[b]</sup>	64/25/11 (isotactic enriched)	this work
3	K[CaA' <sub>3</sub> ] ( <b>2</b> )	1000	-78	8 min	23	29	76,300 <sup>[b]</sup>	10.41 <sup>[b]</sup>	66/28/6 (isotactic enriched)	this work
4	(n-Bu)MgBr	50	-78	72 h	14		7,420	11.2	21/15/64 (syndiotactic enriched)	[44]
5	K[A']	1000	-78	0.5 min	87	1150	–	–	25/53/22 (atactic)	[40]
(B) Polymerization of isoprene										
Entry	Initiator	Mono/ cat	Temp (°C)	Time (h)	Yield (%)	M <sub>n</sub> (g/ mol) <sup>[e]</sup>	Đ <sup>[e]</sup>	1,2/1,4/3,4 <sup>[f]</sup>	Ref.	
6	K[CaA' <sub>3</sub> ] ( <b>2</b> ) <sup>[d]</sup>	200	RT	12	98	16,300 <sup>[e]</sup>	1.27 <sup>[e]</sup>	0/63/37	this work	
7	K[CaA' <sub>3</sub> ] ( <b>2</b> ) <sup>[d]</sup>	200	50	12	99	14,200	1.63	0/64/36	this work	
8	K[CaA' <sub>3</sub> ] ( <b>2</b> ) <sup>[d]</sup>	200	80	12	98	11,400	1.52	0/64/36	this work	
9	K[CaA' <sub>3</sub> ] + 1 eq THF <sup>[d]</sup>	200	RT	12	0	–	–	–	this work	
10	K[A'] <sup>[d]</sup>	200	RT	12	0	–	–	–	this work	
11	[CaA' <sub>2</sub> (thf) <sub>2</sub> ] <sup>[d]</sup>	200	RT	12	0	–	–	–	this work	
12	K[A'] + [CaA' <sub>2</sub> (thf) <sub>2</sub> ] <sup>[d]</sup>	200	RT	12	0	–	–	–	this work	
13	<i>sec</i> -BuLi		80	2	–	39,300	1.04		[46]	
14	(DMAT) <sub>2</sub> Ca(thf) <sub>2</sub>	100	50	1	–	20,600	1.30	22/52/26	[46]	
15	[(DMAT)(9-TMS-FI)Ca] <sub>2</sub>	100	50	0.25	–	15,400	1.26	11/52/37	[46]	

[a] Conditions for initiation with K[CaA'<sub>3</sub>]: 0.25 g monomer, 0.5 M with respect to monomer in toluene, cooled to the respective temperature before monomer addition, then quenched with acidic MeOH and precipitated into MeOH. [b] Number average molecular weights (M<sub>n</sub>) and dispersities (Đ) were measured via GPC at 40 °C in THF, and are reported relative to PMMA standards. [c] Tacticities are reported as percent mm/mr/rr triads as determined from <sup>1</sup>H NMR spectra. [d] Conditions: 0.25 g monomer, 4 mL toluene, quenched with acidic MeOH and precipitated into MeOH. [e] Number average molecular weights (M<sub>n</sub>) and dispersities (Đ) were measured via GPC at 30 °C in THF using triple detection. [f] Tacticities are reported as percent mm/mr/rr triads as determined from <sup>1</sup>H NMR spectra.

In comparison to MMA polymerizations, the polymerization of dienes with *s*-block complexes has received much less study.<sup>[4b]</sup> The stereochemistry and regiochemistry of conjugated diene insertion is more complex than with alkenes. For example, butadiene can give rise to *cis*- and *trans*-1,4-isomers, and the stereocenter generated from 1,2-polymerization of butadiene opens the possibility for isotactic, syndiotactic, and atactic microstructures. Isoprene polymerization is even more complex: 1,4- insertions can lead to *cis*- and *trans*- isomers, and 1,2- and 3,4- insertions generate chiral centers with extra possibilities for microstructural arrangements (Figure 6).

**Figure 6.** Stereochemical possibilities for polyisoprenes.

Calcium and barium complexes have been examined as initiators of butadiene polymerization,<sup>[46]</sup> but studies of isoprene polymerization with the heavy Group 2 elements are rare. The fluorenyl complex {(Me<sub>3</sub>Si-fluorenyl)[*o*-(dimethylamino)benzyl]Ca}<sub>2</sub> [(DMAT)(9-TMS-FI)Ca]<sub>2</sub><sup>[47]</sup> and the benzyl derivative (DMAT)<sub>2</sub>Ca(thf)<sub>2</sub> (DMAT = 2-dimethylamino- $\alpha$ -trimethylsilylbenzyl) have been used as initiators for isoprene polymerization in cyclohexane, and give mixtures of 1,2-/1,4-/3,4-insertion products (entries 14,15).<sup>[48]</sup>

The potassium allyl complex K[A'] was found to be inactive as an initiator for isoprene polymerization (Table 2, entry 10, and the Supporting Information), as was the solvated [CaA'<sub>2</sub>(thf)<sub>2</sub>] (entry 11). However, complex **2** initiates isoprene polymerization in toluene (entry 6) at room temperature and atmospheric pressure, producing polyisoprene in high yield and low dispersity. As a note, these are the mildest conditions yet reported for a heavy Group 2 isoprene polymerization initiator. For polymerizations using initiator **2**, only two insertion products are observed, 1,4- and 3,4- in a 63:37 ratio (see the Supporting Information for details). Repetition of the reaction at 50 °C and 80 °C (entries 7,8) indicate that the initiator remains

active, repeatedly producing yields  $\geq 98\%$ . However, polyisoprene molecular weights ( $M_n$ ) were observed to decrease by 13% at 50 °C, and by 30% at 80 °C, and  $\mathcal{D}$  values increased modestly, by 0.2–0.3. Such a decrease in  $M_n$  is characteristic of increased chain transfer at elevated temperatures, which is also known to broaden dispersity.<sup>[49]</sup>

Finally, the deleterious effect that THF has on the initiating ability should be noted. Addition of an equivalent of THF to a solution of **2** (Table 2, entry 9) completely suppresses any isoprene polymerization activity. Furthermore, the combination of  $K[A']$  and  $[CaA'_2(thf)_2]$  (entry 12) is also inactive, indicating that they do not associate to generate an 'ate'-type species. This underscores the critical importance of the initial solvent-free mechanochemical synthesis for the subsequent reactivity of the  $K[CaA'_3]$  system.

### 3. Conclusion

In addition to its benefits as a 'green' approach to synthesis, mechanochemistry offers a valuable way to generate molecules that are unavailable from solution-based methods. When describing the outcome of a reaction, there is a potential difference between the initial product and the results of the first contact of such species with the solvent(s) during the rest of the reaction time and during workup. Compounds that are prepared and isolated from solvent-based conditions have undergone a type of "selection by solution", and potentially useful molecules can be lost by that initial interaction. Mechanochemically based synthesis, in contrast, permits a separation between an initially formed product and the changes that might occur during a solvent-based workup.<sup>[50]</sup>

The absence of ethers in the attempted synthesis of  $[CaA'_2]$  leads instead, owing to coordinative unsaturation, to the formation of the "ate" complex  $K[CaA'_3]$ . The heterohaptic allyl complex undergoes smooth conversion to a still highly active, all- $\pi$ -bound polymorph. Such behavior highlights a synergy between the solid state and solution environments that likely exists with other heterometallic main group metal complexes, most probably with strontium and barium, and which presents additional possibilities for generating highly active reagents and catalytic initiators.

### 4. Supporting Information

The Supporting Information includes additional experimental and computational details, and optimized coordinates of structures (.xyz format). Deposition Numbers 2024008 (**2**), 2024009 (**2b**), and 2024040 (**2c**) contain the supplementary crystallographic data for this paper. These data are provided free of charge by the joint Cambridge Crystallographic Data Centre and Fachinformationszentrum Karlsruhe Access Structures service [www.ccdc.cam.ac.uk/structures](http://www.ccdc.cam.ac.uk/structures).

### Acknowledgements

Financial support by the National Science Foundation (CHE-1665327), the American Chemical Society–Petroleum Research Fund (56027-ND3), and a Charles M. Lukehart Fellowship (to R.F.K.) is gratefully acknowledged.

### Conflict of Interest

The authors declare no conflict of interest.

**Keywords:** Allyl ligands · Calcium · Mechanochemistry · Polymerization · Potassium

- [1] E. Beckmann, *Ber. Dtsch. Chem. Ges.* **1905**, *38*, 904–906.
- [2] S. Kriek, M. Westerhausen, *Encyclopedia of Inorganic and Bioinorganic Chemistry* (Ed.: R. A. Scott), Wiley, **2015**, pp. 1–17.
- [3] F. A. Cotton, G. Wilkinson, *Advanced Inorganic Chemistry*, 4th ed., Wiley, New York, **1980**, p. 271. The organometallic compounds of calcium, strontium, and barium are described as "relatively obscure and of little utility."
- [4] a) M. Westerhausen, M. Gaertner, R. Fischer, J. Langer, L. Yu, M. Reiher, *Chem. Eur. J.* **2007**, *13*, 6292–6306; b) S. Harder, *Early Main Group Metal Catalysis: Concepts and Reactions*, 1st ed., Wiley-VCH, Weinheim, **2020**; p. 43.
- [5] a) S. Harder, *Angew. Chem. Int. Ed.* **2004**, *43*, 2714–2718; *Angew. Chem.* **2004**, *116*, 2768–2718; b) I. Yildirim, S. Crotty, C. H. Loh, G. Festag, C. Weber, P.-F. Caponi, M. Gottschaldt, M. Westerhausen, U. S. Schubert, *J. Polym. Sci. Part A* **2016**, *54*, 437–448; c) I. Yildirim, T. Yildirim, D. Kalden, G. Festag, N. Fritz, C. Weber, S. Schubert, M. Westerhausen, U. S. Schubert, *Polym. Chem.* **2017**, *8*, 4378–4387.
- [6] a) D. Schuhknecht, C. Lhotzky, T. P. Spaniol, L. Maron, J. Okuda, *Angew. Chem. Int. Ed.* **2017**, *56*, 12367–12371; *Angew. Chem.* **2017**, *129*, 12539–12371; b) H. Bauer, M. Alonso, C. Färber, H. Elsen, J. Pahl, A. Causero, G. Ballmann, F. De Proft, S. Harder, *Nat. Catal.* **2018**, *1*, 40–47; c) J. Martin, C. Knüpfer, J. Eyslein, C. Färber, S. Grams, J. Langer, K. Thum, M. Wiesinger, S. Harder, *Angew. Chem. Int. Ed.* **2020**, *59*, 9102; *Angew. Chem.* **2020**, *132*, 9187–9112.
- [7] a) D. Schuhknecht, T. P. Spaniol, L. Maron, J. Okuda, *Angew. Chem. Int. Ed.* **2020**, *59*, 310–314; *Angew. Chem.* **2020**, *132*, 317–314; b) D. Mukherjee, D. Schuhknecht, J. Okuda, *Angew. Chem. Int. Ed.* **2018**, *57*, 9590–9602; c) P. Jochmann, J. P. Davin, T. P. Spaniol, L. Maron, J. Okuda, *Angew. Chem. Int. Ed.* **2012**, *51*, 4452–4455; d) S. Kriek, D. Kalden, A. Oberheide, L. Seyfarth, H.-D. Arndt, H. Görls, M. Westerhausen, *Dalton Trans.* **2019**, *48*, 2479–2490; e) S. Ziemann, S. Kriek, H. Görls, M. Westerhausen, *Organometallics* **2018**, *37*, 924–933; f) T. M. A. Al-Shboul, H. Görls, M. Westerhausen, *Inorg. Chem. Commun.* **2008**, *11*, 1419–1421; g) F. M. Younis, S. Kriek, T. M. A. Al-Shboul, H. Görls, M. Westerhausen, *Inorg. Chem.* **2016**, *55*, 4676–4682; h) S. Harder, J. Spielmann, *J. Organomet. Chem.* **2012**, *698*, 7–14.
- [8] A. S. S. Wilson, M. S. Hill, M. F. Mahon, C. Dinoi, L. Maron, *Science* **2017**, *358*, 1168–1171.
- [9] a) T. P. Hanusa, *Chem. Rev.* **1993**, *93*, 1023–1036; b) T. P. Hanusa, *Organometallics* **2002**, *21*, 2559–2571; c) S. C. Chmely, T. P. Hanusa, *Eur. J. Inorg. Chem.* **2010**, 1321–1337; d) S. A. Solomon, R. A. Layfield, *Dalton Trans.* **2010**, *39*, 2469–2483; e) C. Lichtenberg, J. Okuda, *Angew. Chem. Int. Ed.* **2013**, *52*, 5228–5246; *Angew. Chem.* **2013**, *125*, 5336–5246.
- [10] R. F. Koby, A. M. Doerr, N. R. Rightmire, N. D. Schley, B. K. Long, T. P. Hanusa, *Angew. Chem. Int. Ed.* **2020**, *59* 9542–9548; *Angew. Chem.* **2020**, *132*, 9629–9548.
- [11] K. T. Quisenberry, R. E. White, T. P. Hanusa, W. W. Brennessel, *New J. Chem.* **2010**, *34*, 1579–1584.
- [12] A. S. S. Wilson, C. Dinoi, M. S. Hill, M. F. Mahon, L. Maron, *Angew. Chem. Int. Ed.* **2018**, *57*, 15500–15504; *Angew. Chem.* **2018**, *130*, 15726–15504.
- [13] S. C. Chmely, C. N. Carlson, T. P. Hanusa, A. L. Rheingold, *J. Am. Chem. Soc.* **2009**, *131*, 6344–6345.
- [14] S. C. Chmely, T. P. Hanusa, W. W. Brennessel, *Angew. Chem. Int. Ed.* **2010**, *49*, 5870–5874.

- [15] a) J. G. Hernández, I. S. Butler, T. Friščić, *Chem. Sci.* **2014**, *5*, 3576–3582; b) J.-L. Do, T. Friščić, *ACS Cent. Sci.* **2017**, *3*, 13–19; c) T. Friščić, C. Mottillo, H. M. Titi, *Angew. Chem. Int. Ed.* **2020**, *59*, 1018–1029; *Angew. Chem.* **2020**, *132*, 1030–1029; d) J. G. Hernández, C. Bolm, *J. Org. Chem.* **2017**, *82*, 4007–4019; e) K. Kubota, R. Takahashi, H. Ito, *Chem. Sci.* **2019**, *10*, 5837–5842; f) Y. Pang, T. Ishiyama, K. Kubota, H. Ito, *Chem. Eur. J.* **2019**, *25*, 4654–4659.
- [16] a) N. R. Rightmire, T. P. Hanusa, A. L. Rheingold, *Organometallics* **2014**, *33*, 5952–5955; b) R. F. Koby, T. P. Hanusa, N. D. Schley, *J. Am. Chem. Soc.* **2018**, *140*, 15934–15942; c) Y. X. Shi, K. Xu, J. K. Clegg, R. Ganguly, H. Hirao, T. Friščić, F. García, *Angew. Chem. Int. Ed.* **2016**, *55*, 12736–12740; *Angew. Chem.* **2016**, *128*, 12928–12740.
- [17] C. Lichtenberg, T. P. Spaniol, I. Peckermann, T. P. Hanusa, J. Okuda, *J. Am. Chem. Soc.* **2013**, *135*, 811–821.
- [18] M. J. Harvey, T. P. Hanusa, V. G. Young, Jr., *Angew. Chem. Int. Ed.* **1999**, *38*, 217–219; *Angew. Chem.* **1999**, *111*, 241–219.
- [19] Stirring 2:1 mixture of K[A] and Cal<sub>2</sub> in toluene overnight leaves only the starting materials (<sup>1</sup>H NMR evidence). This is unsurprising, given the low solubility of K[A] in toluene, and the complete insolubility of Cal<sub>2</sub> in the same. The lack of reaction is also evidence that the formation of K[CaA<sub>3</sub>] from the milled reaction mixture is not simply a result of the workup in toluene.
- [20] N. Boyde, N. Rightmire, T. Hanusa, W. Brennessel, *Inorganics* **2017**, *5*, 36.
- [21] C. K. Gren, T. P. Hanusa, A. L. Rheingold, *Organometallics* **2007**, *26*, 1643–1649.
- [22] C. K. Gren, T. P. Hanusa, W. W. Brennessel, *Polyhedron* **2006**, *25*, 286–292.
- [23] A. J. Bissette, S. P. Fletcher, *Angew. Chem. Int. Ed.* **2013**, *52*, 12800–12826; *Angew. Chem.* **2013**, *125*, 13034–12826.
- [24] Autocatalysis is possible if the induction period reflects rapid interconversion between various polymorphs of solvated **1** (see ref. [23] for the underlying theory). Several speculative intermediates are possible (see the Computational Results section for examples), but constructing a catalytic cycle would require more conjecture, the validity of which would be extremely difficult, if not impossible, to judge.
- [25] K. T. Quisenberry, J. D. Smith, M. Voehler, D. F. Stec, T. P. Hanusa, W. W. Brennessel, *J. Am. Chem. Soc.* **2005**, *127*, 4376–4387.
- [26] C. K. Simpson, R. E. White, C. N. Carlson, D. A. Wroblewski, C. J. Kuehl, T. A. Croce, I. M. Steele, B. L. Scott, T. P. Hanusa, A. P. Sattelberger, K. D. John, *Organometallics* **2005**, *24*, 3685–3691.
- [27] L. Pauling, *The Nature of the Chemical Bond*, 3rd. ed., Cornell University Press, Ithaca, **1960**, p. 260.
- [28] Methylcyclopentane comprises about 10% of commercial hexanes mixtures (Oakwood Chemicals). Its boiling point of 72 °C (cf. 69 °C for *n*-hexane) means that it is not routinely separated from other C<sub>6</sub> alkanes. It might be noted that there are 52 methylcyclopentane solvates in the CCSD (Nov. 2020 release).
- [29] J. L. Howard, M. C. Brand, D. L. Browne, *Angew. Chem. Int. Ed.* **2018**, *57*, 16104–16108; *Angew. Chem.* **2018**, *130*, 16336–16108.
- [30] K. Užarević, I. Halasz, T. Friščić, *J. Phys. Chem. Lett.* **2015**, *6*, 4129–4140.
- [31] a) K. Užarević, N. Ferdelji, T. Mrla, P. A. Julien, B. Halasz, T. Friščić, I. Halasz, *Chem. Sci.* **2018**, *9*, 2525–2532; b) I. R. Speight, I. Huskić, M. Arhangelskis, H. M. Titi, R. S. Stein, T. P. Hanusa, T. Friščić, *Chem. Eur. J.* **2020**, *26*, 1811–1816.
- [32] I. Halasz, S. A. J. Kimber, P. J. Beldon, A. M. Belenguer, F. Adams, V. Honkimäki, R. C. Nightingale, R. E. Dinnebier, T. Friščić, *Nat. Protoc.* **2013**, *8*, 1718–1729.
- [33] T. Friščić, I. Halasz, P. J. Beldon, A. M. Belenguer, F. Adams, S. A. J. Kimber, V. Honkimäki, R. E. Dinnebier, *Nat. Chem.* **2013**, *5*, 66–73.
- [34] D. Gracin, V. Štrukil, T. Friščić, I. Halasz, T. Užarević, *Angew. Chem. Int. Ed.* **2014**, *53*, 6193–6197.
- [35] a) L. Bätzdorf, F. Fischer, M. Wilke, K. J. Wenzel, F. Emmerling, *Angew. Chem. Int. Ed.* **2015**, *54*, 1799; *Angew. Chem.* **2015**, *127*, 1819–1802; b) S. Lukin, T. Stolar, M. Tireli, M. V. Blanco, D. Babić, T. Friščić, K. Užarević, I. Halasz, *Chem. Eur. J.* **2017**, *23*, 13941–13949.
- [36] a) J. P. Gallivan, D. A. Dougherty, *Proc. Nat. Acad. Sci. USA* **1999**, *96*, 9459–9464; b) Y.-H. Cheng, L. Liu, Y. Fu, R. Chen, X.-S. Li, Q.-X. Guo, *J. Phys. Chem. A* **2002**, *106*, 11215–11220.
- [37] J. Tomasi, B. Mennucci, R. Cammi, *Chem. Rev.* **2005**, *105*, 2999–3094.
- [38] P. Jochmann, T. P. Spaniol, S. C. Chmely, T. P. Hanusa, J. Okuda, *Organometallics* **2011**, *30*, 5291–5296.
- [39] P. B. Hitchcock, A. V. Khvostov, M. F. Lappert, *J. Organomet. Chem.* **2002**, *663*, 263–268.
- [40] a) L. Quisenberry, C. K. Gren, R. E. White, T. P. Hanusa, W. W. Brennessel, *Organometallics* **2007**, *26*, 4354–4356; b) T. J. Woodman, M. Schormann, D. L. Hughes, M. Bochmann, *Organometallics* **2004**, *23*, 2972–2979.
- [41] R. E. White, *PhD thesis*, Vanderbilt University (Nashville, TN), **2006**.
- [42] W.-F. Su, *Principles of Polymer Design and Synthesis*, Springer, Heidelberg, **2013**, pp. 185–218.
- [43] a) A. Parry, *Reactivity, Mechanism and Structure in Polymer Chemistry* (Eds.: A. D. Jenkins, A. Ledwith), Wiley, London, **1974**, pp. 350–382; b) L. S. Boffa, B. M. Novak, *Transition Metal Catalysis in Macromolecular Design*, Oxford University Press, Washington, DC, **2000**.
- [44] a) M. Szwarc, *Advances in Polymer Science*, Vol. 49, Springer, **1983**, pp. 1–177; b) K. Hatada, H. Nakanishi, K. Ute, T. Kitayama, *Polym. J.* **1986**, *18*, 581–591; c) K. Hatada, T. Shinozaki, K. Ute, T. Kitayama, *Polym. Bull.* **1988**, *19*, 231–237.
- [45] K. Hatada, K. Ute, K. Tanaka, Y. Okamoto, T. Kitayama, *Polym. J.* **1986**, *18*, 1037–1047.
- [46] a) P. Jochmann, T. S. Dols, T. P. Spaniol, L. Perrin, L. Maron, J. Okuda, *Angew. Chem. Int. Ed.* **2009**, *48*, 5715; *Angew. Chem.* **2009**, *121*, 5825–5719; b) B. I. Nakhmanovich, R. V. Basova, A. A. Arest-yakubovich, *J. Macromol. Sci. Part A* **1975**, *9*, 575–596; c) Michelin et Cie (Comp. General. Etabl. Michelin), **1971**.
- [47] S. Harder, F. Feil, *Organometallics* **2002**, *21*, 2268–2274.
- [48] F. Feil, *PhD thesis*, Universität Konstanz **2002**.
- [49] L. Friebe, O. Nuyken, W. Obrecht, *Neodymium Based Ziegler Catalysts – Fundamental Chemistry* (Ed.: O. Nuyken), Springer, Heidelberg, **2006**, pp. 1–154.
- [50] Workup in solution is not an absolute necessity. The product may be formed with essentially no by-products (D. Tan, L. Loots and T. Friščić, *Chem. Commun.*, **2016**, *52*, 7760–7781), or it might be purified by a solvent-free method, e.g., sublimation. Small amounts of solvents are often required, however, for the workup of organometallic compounds prepared with grinding or milling.

Manuscript received: February 15, 2021  
Accepted manuscript online: April 1, 2021  
Version of record online: April 27, 2021